Journal of Colloid and Interface Science 344 (2010) 61–69

Contents lists available at ScienceDirect

Journal of Colloid and Interface Science

www.elsevier.com/locate/jcis

Thermally-triggered gelation of PLGA dispersions: Towards an injectable colloidal cell delivery system

Michael R. Fraylich [a], Ruixue Liu [a,b], Stephen M. Richardson [c], Pauline Baird [c], Judith Hoyland [c], Anthony J. Freemont [c], Cameron Alexander [d], Kevin Shakesheff [d], Francesco Cellesi [e], Brian R. Saunders [a,*]

[a] Biomaterial Science Group, School of Materials, The University of Manchester, Grosvenor Street, Manchester M1 7HS, UK
[b] School of Material and Chemical Engineering, Zhengzhou University of Light Industry, Zhengzhou 450002, PR China
[c] Tissue Injury and Repair Group, School of Clinical and Laboratory Sciences, Faculty of Medical and Human Sciences, Oxford Road, Manchester M13 9PT, UK
[d] School of Pharmacy, Boots Science Building, University of Nottingham, University Park, Nottingham NG7 2RD, UK
[e] Laboratory of Polymers and Biomaterials, School of Pharmacy, The University of Manchester, Oxford Road, M13 9PT, UK

ARTICLE INFO

Article history:
Received 2 November 2009
Accepted 15 December 2009
Available online 22 December 2009

Keywords:
Isopropylacrylamide
Thermoresponsive
Thermogelling
PLGA dispersions

ABSTRACT

In this study the properties of poly(D,L-lactide-*co*-glycolide) (PLGA) dispersions containing a thermoresponsive cationic copolymer were investigated. The PLGA dispersions were prepared by interfacial deposition in aqueous solution and were rendered thermoresponsive by addition of a cationic poly(*N*-isopropyl acrylamide) (PNIPAm) graft copolymer. The copolymers used had the general composition $PDMA_x^+$-*g*-$(PNIPAm_n)_y$. DMA^+ is quarternarized *N*,*N*-dimethylaminoethyl methacrylate. The $PDMA_x^+$-*g*-$(PNIPAm_n)_y$ copolymers have *x* and *y* values that originate from the macroinitiator used for their preparation; values for *n* correspond to the PNIPAm arm length. The thermoresponsive dispersions were characterised using photon correlation spectroscopy, turbidity measurements and electrophoretic mobility measurements. A strong electrostatic attraction between the anionic PLGA particles and cationic copolymer was present and the dispersions showed thermally-triggered gelation at total polymer volume fractions as low as 0.015. These new PLGA gels, which formed at about 32 °C, had elastic modulus values that could be controlled using dispersion composition. Scanning electron micrographs of the gels showed high porosity and interconnectivity of elongated pores. Remarkably, the gels were flexible and had critical yield strains as high as 160%. The ability of the gels to support growth of bovine nucleus pulposus cells was investigated using two-dimensional cell culture. The cells proliferated and remained viable on the gels after 3 days. The results suggest that this general family of biodegradable thermogelling PLGA dispersions, introduced here for the first time, may have longer-term application as an injectable colloidal cell delivery system.

1. Introduction

Thermoresponsive dispersions can form gels when heated and are attracting increased attention [1–5]. They are academically interesting because of fundamental questions concerning the role of interparticle forces and aggregation in network elasticity [4]. They are also of interest for potential application as minimally-invasive, injectable, cell delivery systems [6]. Recently, it was shown that micrometre-sized poly(lactic acid-*co*-glycolic) acid (PLGA) particles could be rendered thermoresponsive by addition of a thermoresponsive copolymer [6]. Those particle gels required high particle PLGA concentrations (up to 60 wt.%) for thermally-triggered gelation and were brittle. Here, a new general approach for the preparation of thermogelling PLGA dispersions is presented. The gels studied here are prepared using nanometre-sized PLGA particles, a cationic thermoresponsive copolymer surfactant and much lower PLGA concentrations. PLGA gels with low particle concentrations could offer improved starting conditions for injectable colloidal cell delivery systems. In earlier work it was found that a cationic poly(*N*-isopropylacrylamide) (PNIPAm) graft copolymer was able to give thermally-triggered gel formation of anionic clay dispersions at low particle concentrations [3]. A related approach was used here with the aim of investigating a new class of thermogelling PLGA dispersion that have potential longer-term application as injectable cell delivery systems.

Although thermoresponsive polymers are well known [7–9], and have been reviewed in detail elsewhere [10], there has been much less work reported involving the use of thermoresponsive polymer surfactants. Careful design of copolymer structure can provide thermoresponsive polymer surfactants that confer triggered gelation to emulsions [11], latexes [12] and inorganic

* Corresponding author. Address: Materials Building, School of Materials, The University of Manchester, Grosvenor St, Manchester, M1 7HS, UK. Fax: +44 (0)161 306 3586.
E-mail address: Brian.saunders@manchester.ac.uk (B.R. Saunders).

0021-9797/$ - see front matter © 2009 Elsevier Inc. All rights reserved.
doi:10.1016/j.jcis.2009.12.030

particle dispersions [3]. Those studies complement related work for thermogelling food colloids [4] and protein dispersions [5]. Compared to macromolecular gels, particle gels tend to be brittle and exhibit structure breakdown at low strains [2]. The essential step in formation of a space-filling particle gel is achieving the correct balance between phase separation on one hand and aggregation and gelation on the other [5]. In the present study we use a cationic thermoresponsive copolymer and anionic particles for this purpose.

PLGA is a well-established biodegradable biomaterial [13]. It has been used in colloidal commercial biomedical devices, such as Lupron depot [14]. Fessi et al. were the first to prepare PLGA dispersions containing nanometre-sized particles using the interfacial deposition method [15]. That method involves addition of a PLGA/solvent solution to a water phase that may, or may not, contain a stabilizing polymer [15–17]. The solvent (e.g., acetone) contains the polymer (e.g., PLGA) and is miscible with water; whereas, the polymer is not water-soluble. Diffusion of the solvent into the water phase results in rapid particle formation. Interfacial turbulence is believed to occur as the solvent rapidly diffuses into the water phase, taking dissolved polymer along with it. This results in deposition of the polymer at the transient acetone/water interface. The particles prepared by this method tend to be polydisperse [15,17]. Interfacial deposition is used in the present work to prepare nanometre-sized PLGA particles.

The ability to render PLGA nanoparticle dispersions thermoresponsive requires a suitable polymer surfactant. Here, we use a cationic PNIPAm graft copolymer [18] (see Scheme 1). The thermoresponsive dispersions are formed simply by mixing mixtures of PLGA and $PDMA^{+}_{x}$-*g*-$(PNIPAm_n)_y$. (DMA^+ is quarternarized *N*,*N*-dimethylaminoethyl methacrylate) The copolymers have *x* and *y* values that originate from the macroinitiator (MI) used for their preparation; values for *n* correspond to the PNIPAm arm length. The abbreviation of [18] MIx-PNIPAm is used for this copolymer from this point onward. The symbol "*x*" signifies that there are approximately *x* positive charges per PNIPAm side chain. The number-average molar mass for each PNIPAm side chain used in the present work [18] is ca. 20 kg mol^{-1}. Pure MIx-PNIPAm solutions are thermogelling [19]. The MIx-PNIPAm copolymers are used here to test the new concept of using a cationic thermoresponsive copolymer to deliver an injectable gel-forming particle dispersion that is biocompatible and biodegradable. The use of PNIPAm copolymers within biomaterials is not, however, proposed here. Rather, it is the use of the general thermoresponsive cationic graft copolymer structure type that is tested.

The developing field of regenerative medicine is reliant on new materials that deliver cells to the point of need and support suitable starting conditions [20]. There is considerable need for biodegradable, injectable cell delivery systems for soft tissue repair because they offer minimally-invasive alternatives to surgery. The dispersions investigated here form gels at much lower particle concentrations than previously investigated [6], show biocompatibility and are mechanically flexible.

2. Experimental

2.1. Materials

A standard phosphate buffer solution [21] with a pH of 7.0 and ionic strength of 0.12 M was used for all experiments presented here except the preparation of the thermogelling dispersions for SEM (Fig. 8) and cell viability studies (Fig. 9). For the latter, PBS (phosphate buffered saline) supplied by Medicago was used (pH = 7.4 and ionic strength of 0.15 M). The PLGA used contained a 75:25 mol ratio of lactide to glycolide units and was a gift from AstraZeneca UK. GPC analysis gave a M_n value of 3140 g mol^{-1} and a polydispersity of 3.0. The synthesis and characterisation of the MI (Scheme 1) and the PNIPAm copolymers used in this study were described fully earlier [18]. Briefly, MI is a statistical copolymer [22], prepared by ATRP (atom transfer radical polymerisation) and contains an average of 1, 2 or 3 positive charges per isobutyrate side chain [18] depending on the composition used during synthesis. The MIx-PNIPAm copolymers (Scheme 1) were prepared by aqueous ATRP using the respective MI. The copolymers were shown previously [18] to have the compositions given in Table 1.

2.2. PLGA nanoparticle preparation

The PLGA dispersions were prepared using interfacial precipitation [15,17,23] according to our previous method [17]. Briefly, acetone and water were cooled to ca. 0 °C in an ice-water bath prior to dispersion preparation. A suitable quantity of PLGA (e.g., 0.16 g) was dissolved in 5.0 ml acetone. This solution was added dropwise to 10 ml of aqueous solution (containing standard phosphate buffer or PBS) over a period of about 5 min at a uniform rate whilst stirring. The dispersion was then rotary evaporated to remove the acetone. The aqueous PLGA dispersion (e.g., containing 1.6 wt.% PLGA) was then mixed with a suitable volume of concentrated aqueous MIx-PNIPAm solution (e.g., 3.2 wt.% MIx-PNIPAm in standard buffer or PBS) to give the desired final PLGA/MIx-PNIPAm

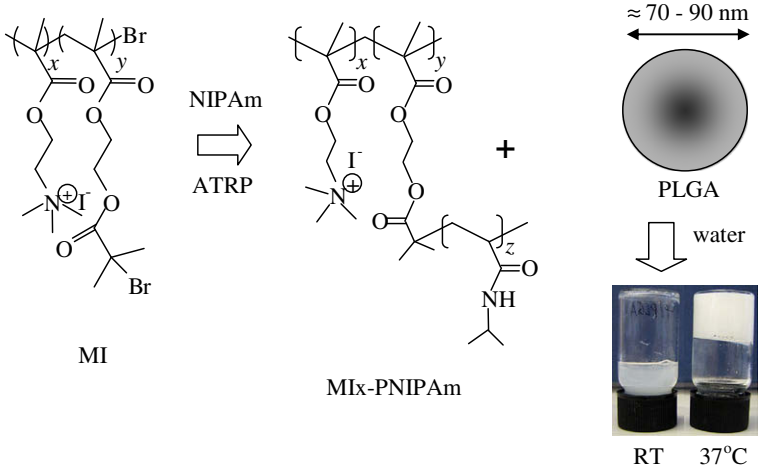

Scheme 1. Preparation of cationic graft copolymer using a macroinitiator (MI) and its use to prepare thermogelling PLGA dispersions.

Table 1
Characterisation data for MIx-PNIPAm copolymers.

Abbreviation	Composition	x/y	M_n/g mol^{-1}	T_{clpt}/°C[a]
MI1-PNIPAm	$PDMA^{+}_{23}$-g-$(PNIPAm_{195})_{23}$	1.0	515,000	29.4
MI2-PNIPAm	$PDMA^{+}_{30}$-g-$(PNIPAm_{210})_{14}$	1.9	348,000	29.0
MI3-PNIPAm	$PDMA^{+}_{37}$-g-$(PNIPAm_{195})_{12}$	3.0	280,000	29.5

[a] The cloud point temperature was taken at the onset of the turbidity increase.

composition. The composition of the dispersions are identified by giving the wt.% of solid present in the water phase in brackets, e.g., PLGA(1.0%)/MI2-PNIPAm(2%) contained 1.0 and 2.0 wt.% of each component.

2.3. Physical measurements

The determination of the cloud point temperature (T_{clpt}) of the copolymer solutions was conducted with a Hitachi U-1800 spectrophotometer using a wavelength of 400 nm and thermostatic control. Particle aggregation was investigated by monitoring the turbidity (τ) and the magnitude of the wavelength exponent, n. [24] This value was obtained from the gradient of the log(τ) versus log(λ) plot ($n = -\mathrm{dlog}(\tau)/\mathrm{dlog}(\lambda)$). The turbidity was measured using UV–visible spectroscopy over the wavelength (λ) range 400–700 nm. The magnitude of n decreases significantly when aggregation occurs [24,25]. SEM was conducted using a Philips FEGSEM instrument. Gel samples were dried onto an SEM specimen stub using a vacuum oven at 39 °C. Photon correlation spectroscopy (PCS) measurements [26] were performed using a Brookhaven BI-9000 light-scattering apparatus fitted with a 20 mW HeNe laser. The detector was set at a 90° scattering angle. A single exponential function was used to fit the data presented here. Electrophoretic mobility measurements were performed using Zetasizer Nano ZS (Malvern Instrument Ltd.). Zeta potentials were calculated using the von Smoluchowski equation [27]. Gelation temperatures were determined using the tube inversion method. The internal diameter of the tubes was ca. 17 mm. Dynamic rheology measurements were performed using a TA instrument AR G2 temperature-controlled rheometer with an environmental chamber. A 20 mm diameter plate geometry with a solvent trap was used. The gap was 1000 nm. A frequency range of 0.5–30 rad s^{-1} was employed. The strain employed was 1.0% unless otherwise stated.

2.4. Cell viability

Cell viability was investigated using a Live/Dead® viability kit (Molecular Probes, Inc.) according to the manufacturer's instructions. The cells used in this study were bovine nucleus pulposus (NP) cells isolated from caudal intervertebral discs and cultured using standard protocols. For all experiments sterile conditions were used. Collagen gels (used as a control) were prepared from solutions of rat type I collagen in acetic acid (Arthro Kinetics Plc), which when mixed with a neutralising solution in cell culture medium rapidly formed a gel. Gels were formed in 24-well plates, with approximately 2 ml of gel in each well. Once formed, 10^5 cells were seeded on the surface of all gels and cultured with 1 ml cell culture medium for 72 h. At selected time points the media was removed and the cells incubated for 30 min with 4 μM ethidium homodimer-1 and 2 μM calcein-AM fluorescent dyes in phosphate buffered saline. As calcein-AM is cell membrane permeable all cells stained green; whereas, ethidium homodimer-1 is cell membrane impermeable and was only absorbed by dead or dying cells following disruption of their membranes. The gels were imaged at 37 °C using a Leica MZ16FA stereo fluorescence microscope with images acquired through Hammamatsu software and a C8484–05g014 camera. The appropriate red or green filters were used to capture the images. The red[1] and green images were then superimposed to yield the final live/dead images.

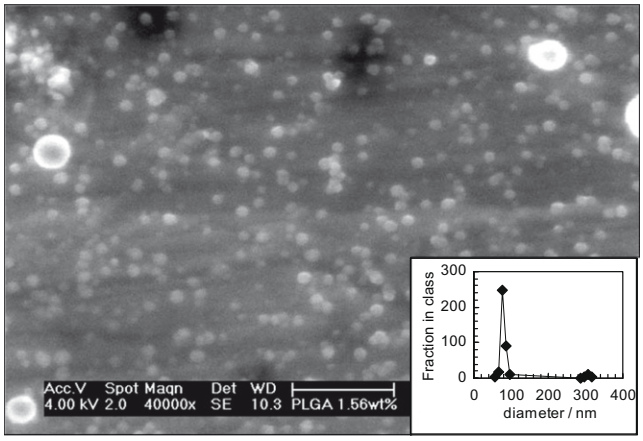

Fig. 1. SEM micrograph of PLGA particles. The scale bar represents 500 nm. The inset shows the particle size distributions.

3. Results and discussion

3.1. Dilute PLGA/MIx-PNIPAm dispersion properties

A representative SEM image of the as-made PLGA particles is shown in Fig. 1. The number-average diameter was 87 nm. The majority of the particles had sizes in the range 70–90 nm. As can be seen from the particle size distribution (inset of Fig. 1) a minor fraction of all the particles (ca. 0.05) had a larger size, of about 300 nm. We have found interfacial deposition of PLGA to give bimodal particle size distributions and even coagulation at high concentrations [17]. In the present work a balance was sought between producing relatively high particle concentrations and minimising coagulation.

The interactions between the dispersed PLGA particles and added MIx-PNIPAm were investigated using electrophoretic mobility and PCS measurements (Fig. 2). The double layer thickness (κ^{-1}) for the dispersions was ca. 9 nm. From Fig. 2a it can be seen the zeta potential (ζ) of the bare PLGA nanoparticles was around −63 mV, which is attributed to $RCOO^-$ groups formed by hydrolysis of PLGA [13]. Addition of MIx-PNIPAm to the PLGA dispersions decreased the magnitudes of the zeta potentials. For PLGA particles in the presence of MI1-PNIPAm or MI2-PNIPAm the isoelectric point (*iep*) occurred at about 0.012 wt.% of added copolymer. It was higher (ca. 0.017 wt.%) in the presence of MI3-PNIPAm. The PLGA particles did not become positively charged at high polymer concentration, which differs to the behaviour reported for linear polyelectrolytes adsorbed onto polystyrene particles where overcompensation occurred [28]. A reason for this is suggested later.

In the absence of added MIx-PNIPAm the hydrodynamic diameter (d_h) for the PLGA particles (Fig. 2b) was 200 nm. This is much larger than the diameter obtained from SEM (87 nm). PCS calculates a *z*-average particle size. For comparison, the *z*-average particle size was calculated from the SEM particle size distribution given in the inset of Fig. 1 using the following equation [29].

$$d_z = \frac{\sum_i n_i d_i^3}{\sum_i n_i d_i^2} \quad (1)$$

[1] For interpretation of color in Fig. 9, the reader is referred to the web version of this article.

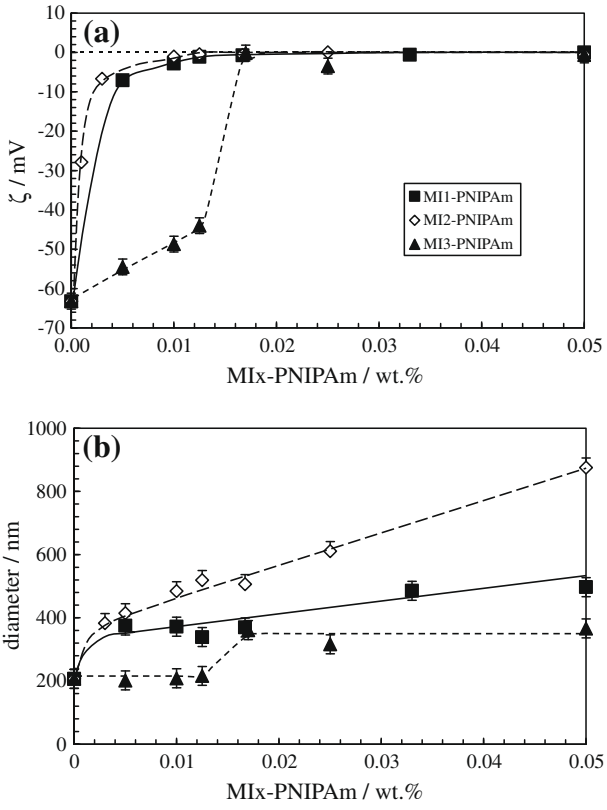

Fig. 2. Zeta potential: (a) and hydrodynamic diameter (b) as a function of concentration of added copolymer present for a dispersion containing 0.195 wt.% PLGA nanoparticles. The lines are guides for the eye. The measurements were conducted at 25 °C.

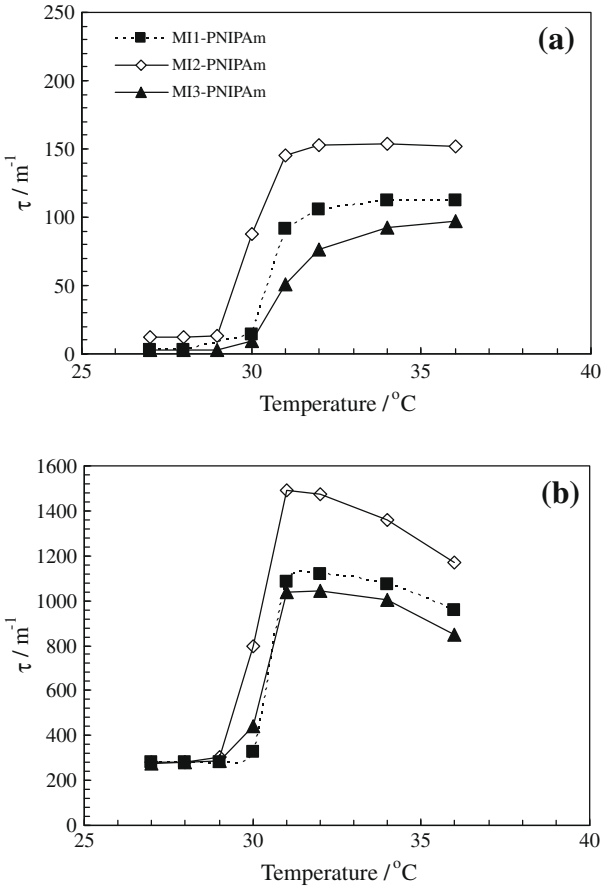

Fig. 3. Temperature dependence of turbidity for (a) MIx-PNIPAm solutions and (b) PLGA(0.0244%)/MIx-PNIPAm(0.00625%) dispersions.

Using Eq. (1) a value for d_z of 172 nm was calculated. This value is reasonably close to the d_h value and supports the view that the PCS data give meaningful average particle sizes in the dispersed state. The PCS data are useful for probing subtle changes in dispersion stability upon addition of MIx-PNIPAm. The d_h values for the PLGA/MI3-PNIPAm system increased sharply at the *iep* (0.017 wt.%) and were then constant. In contrast the PLGA/MI1-PNIPAm and PLGA/MI2-PNIPAm mixtures showed continual increases in d_h beyond their *iep* values (ca. 0.012 wt.%). The relatively large increases in d_h values for the latter two dispersions imply aggregation. However, it is important to note that the dispersions did *not* show visual evidence of aggregation at room temperature. They existed as free-flowing liquids and were readily injectable through narrow gauge syringe needles.

Turbidity-wavelength measurements were used to further probe particle aggregation (Data shown in Fig. S1). A decrease in the magnitude of n is indicative of pronounced aggregation [24,25]. Importantly, the values for n were constant across the entire MIx-PNIPAm concentration range probed in Fig. 2. Large-scale PLGA aggregation did not occur for these systems at 25 °C. On balance, the visual and light-scattering data (Fig. 2b and Fig. S1) point to limited aggregation for these systems, i.e., the formation of small aggregates at 25 °C. The tendency for (limited) aggregate formation at 25 °C increased in the order MI3-PNIPAm < MI1-PNIPAm < MI2-PNIPAm. It is assumed that coverage of the particles by the copolymer occurred at the *iep* values. For the remainder of the study the concentration ratios of MIx-PNIPAm to PLGA used exceeded those required for the respective *iep* values (Fig. 2a).

The PNIPAm copolymers are thermoresponsive and the turbidity of the pure solutions increased beyond the T_{clpt} value (see Fig. 3a). (The T_{clpt} values shown in Table 1 were taken from the onset of the thermally-triggered turbidity increase.) The T_{clpt} values are about 4 °C lower than those reported in an earlier study where added buffer was not used [18]. For the data shown in Fig. 3 the buffer had an ionic strength of about 0.12 M and this decreased the T_{clpt} values due to electrostatic screening.

Visual observations for PLGA(0.0244%)/MIx-PNIPAm(0.00625%) dispersions revealed substantial aggregation upon heating. This was investigated in more detail using variable-temperature turbidity measurements (Fig. 3b). Variable temperature turbidity-wavelength analysis was also used for comparison (see Fig. S2). The critical flocculation temperature (CFT) was taken as the onset of the increase in τ (Fig. 3b) and decrease in the magnitude of n (Fig. S2). Similar CFTs were the obtained using both turbidity and turbidity-wavelength data analyses. The CFT was 29.0 °C for PLGA/MI2-PNIPAm20k. The CFTs for PLGA/MI1-PNIPAm20k and PLGA/MI3-PNIPAm20k were both 30.0 °C. The values are very close to the T_{clpt} values for the parent copolymers (Table 1). These data imply that LCST variation through structural modification for these thermoresponsive copolymers could be used to pre-programme CFTs for the responsive PLGA dispersions.

The fact that each of these dispersions exhibit thermally-triggered aggregation (Fig. 3b and Fig. S2) shows that any steric stabilisation is removed at temperatures greater than T_{clpt}. Because this occurred at pH = 7.0, at electrolyte concentrations similar to that in the body, the data suggest that PLGA/MIx-PNIPAm dispersions have potential application (in principle) as injectable cell delivery systems. However, the dispersions would be required to form biocompatible gels when heated to body temperature. These aspects are investigated below.

3.2. Thermally-triggered gelation of concentrated PLGA/MIx-PNIPAm dispersions

Concentrated PLGA/MI2-PNIPAm dispersions exhibited thermally-triggered gelation as shown in Scheme 1. Dynamic rheology was used to probe thermally-triggered gelation of PLGA(1%)/MI2-PNIPAm(2%) dispersions. Frequency sweeps for G' (elastic modulus) and tan δ (=G''/G', where G'' is the loss modulus) at different temperatures are shown in Fig. 4. Gels are indicated by tan δ values less than 1.0. Accordingly, the dispersion was a very weak gel at room temperature. However, it was too weak to be detected by tube inversion (later) and flow occurred. It can be seen that the G' and tan δ values increased and decreased, respectively, when the temperature reached 33 °C. The gradients for the G' vs. ω data (Fig. 4a) also decreased significantly at temperatures greater than or equal to 33 °C and obeyed the relationship $G' \sim \omega^{0.1}$. This, coupled with the relatively modest G' values (and tan $\delta < 1$), indicates soft gel behaviour. Soft gels are expected since the total polymer volume fraction was only about 0.03 and the gel relied upon hydrophobic interactions. The PLGA particles are themselves soft and a glass transition temperature in the vicinity of about 40 °C is expected [30].

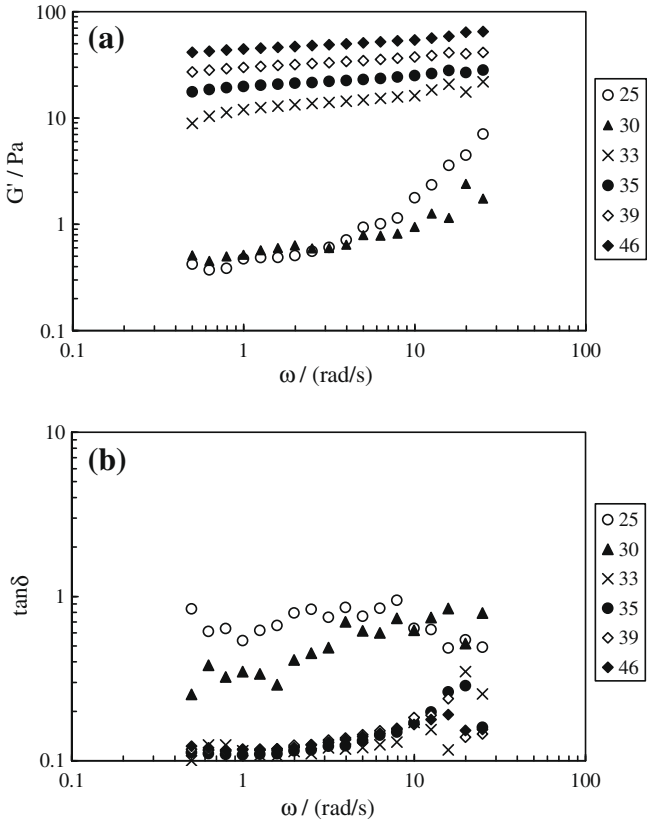

Fig. 4. Variation of G' and tan δ with oscillation frequency for PLGA(1%)/MI2-PNIPAm(2%) dispersions measured at different temperatures. The temperatures (°C) used for the experiments are shown in the legend.

The effect of dispersion composition on the temperature-dependence of G' and tan δ was also investigated (see Fig. 5). The MIx-PNIPAm copolymers with the lowest charge density, MI1-PNIPAm and MI2-PNIPAm, gave the strongest PLGA/MIx-PNIPAm gels, as judged by higher G' and lower tan δ values (Fig. 5a and b) at elevated temperatures. In the case of PLGA/MI3-PNIPAm dispersions (which have lower G' values), stronger inter-segment electrostatic repulsion may have reduced the number density of thermoassociative crosslinks that could form at temperatures greater than T_{clpt}.

It can also be seen from Fig. 5c and d that the presence of PLGA results in a major improvement of the elastic behaviour of the gels, as evidenced by the increase in G' values and decrease in tan δ. This strongly implicates PLGA nanoparticles as cross linking centres within the gels. These data are also important because they show that a major decrease in gel elasticity could be expected if the PLGA nanoparticles were to biodegrade. The value for G' at 39 °C is 40 Pa for PLGA(1%)/MI2-PNIPAm(2%) gel compared to 4 Pa for MI2-PNIPAm(2%). This indicates a possible application for these materials. If the dispersion could initially be gelled in the presence of cells in vivo, then a cell-polymer aggregate matrix could be established, while upon degradation of the cross linking centres i.e. the PLGA cores, the resultant gel would be very weak and could release the cells in the presence of very low shear. This is support for the principle of a thermogelling cell delivery system.

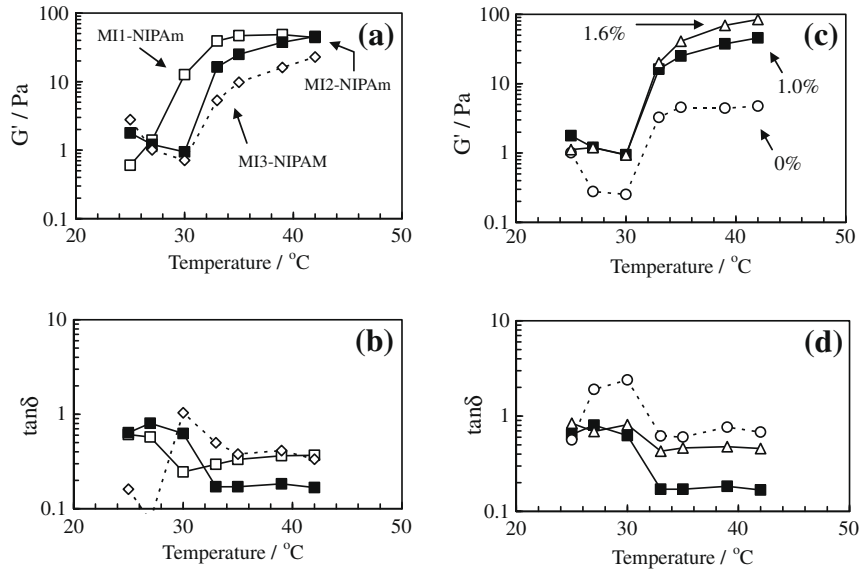

Fig. 5. Variable-temperature G' (upper) and tan δ (lower) dynamic rheology data for PLGA/MIx-PNIPAm dispersions. The effect of copolymer type is shown in (a) and (b) for PLGA(1 wt.%)/MIx-PNIPAm(2 wt.%) dispersions. The effect of PLGA concentration is shown in (c) and (d) where data for PLGA/MI2-PNIPAm(2%) are shown. Data for PLGA(1.6%)/MI2-PNIPAm(3%) are also shown (open triangles). All of the data were obtained at an oscillation frequency of 10 rad/s.

An important aspect from the viewpoint of mechanical property tunability is the effect of MIx-PNIPAm concentration. The elasticity of the dispersion can be increased by increasing the concentration of thermoresponsive copolymer (Fig. S3a and b). A doubling of the MI2-PNIPAm concentration increased the elastic modulus by a factor of five at 39 °C. Values of up to 250 Pa were achieved for PLGA(1%)/MI2-PNIPAm(4%). This must be due to an increased number density of thermoassociative crosslinks within the gels.

The effect of copolymer type on the gelation temperatures (T_{gel}) was also investigated using tube inversion measurements (see Fig. 6a). For these measurements gelation corresponds to the elasticity of the gels becoming sufficiently strong to support their own weight. The T_{gel} values for the PLGA/MIx-PNIPAm dispersions were comparable. The data from Fig. 6b shows that the presence of the PLGA particles substantially decreases the T_{gel} values for the PLGA/MI1-PNIPAm dispersions compared to that of the parent MI1-PNIPAm solution. The PLGA particles behave as interactive fillers [31]. The PLGA particles must act as crosslinking sites. It is potentially important that for a range of compositions and temperatures, the gel state for PLGA(1%)/MI1-PNIPAm can only exist when PLGA particles are present. This region of the phase diagram is shaded in Fig. 6b. This implies that gel-to-fluid transitions could occur over time in vivo, in principle, upon PLGA biodegradation if the local shear were similar to that present during the tube inversion measurements.

A new feature concerning these thermally-triggered PLGA gels compared to earlier work [6], is that the PLGA/MIx-PNIPAm gels form at very low total solid concentrations. For example, from Fig. 6b it can be seen that a gel formed from the PLGA(1.0%)/MI1-PNIPAm(0.5%) dispersion. That system contained about 98.5 vol.% water. This suggests a highly porous gel structure and could be advantageous for nutrient flow.

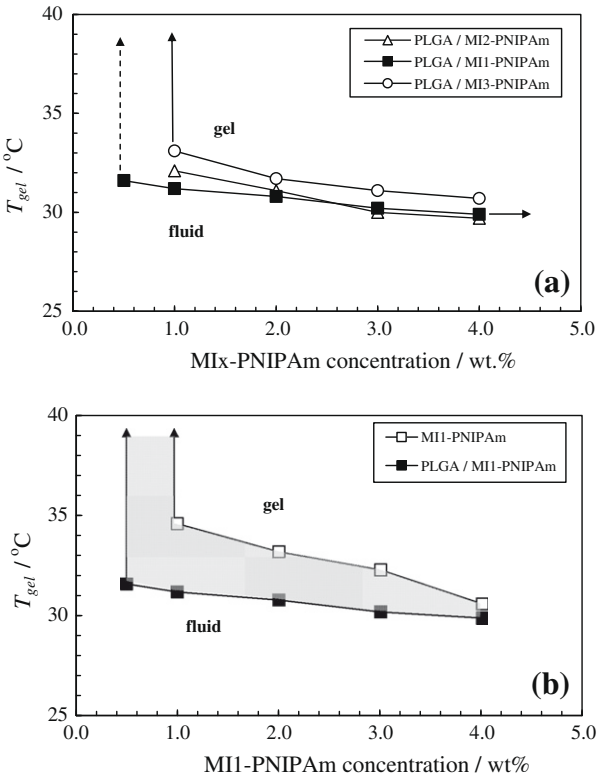

Fig. 6. Gelation phase diagrams for (a) PLGA(1%) dispersions containing added MIx-PNIPAm ($x = 1$, 2 or 3) and (b) PLGA(1%)/MI1-PNIPAm and pure MI1-PNIPAm solution. The shaded region in (b) shows the temperature and composition ranges of the PLGA(1%)/MI1-PNIPAm gel for which PLGA particles are essential for gel formation under the conditions used for the tube inversion measurements.

An interesting question concerns the role of particle size polydispersity on the rheological behaviours discussed above. Although this was not explicitly investigated in this study (e.g., by separating the particles from the smaller particles), we can make some general comments. Firstly, SEM of the particle gels (below) did not show any of the larger particles. Therefore, the rheological behaviours observed above are probably dominated by the smaller particles. More generally, particle gel elasticity is an increasing function of the number of elastically effective (particle) chains per unit volume and the cohesiveness of the particles. Particle gels are predominantly enthalpic in thermodynamic terms with the major contribution being the interparticle interaction energy [32]. Polydispersity should increase the number of elastically effective chains because it increases the total number of particles present, giving a larger number of smaller particles. However, the smaller particles will have a smaller attractive van der Waals interaction energy [33] and potentially lower cohesiveness. A detailed experimental study would therefore be required to resolve this issue. This is beyond the scope of the present study.

3.3. Gel morphology, mechanical flexibility and cell viability

In the final part of the study we sought to assess the potential of using this new class of thermoresponsive dispersions as an injectable cell delivery system. It is understood that PNIPAm may have limited potential as a biomaterial [34,35]. Nevertheless, our MIx-PNIPAm copolymers are a useful structural model for designing thermoresponsive copolymers for future cell delivery applications. Here, we use PLGA/MIx-PNIPAm dispersions to test the new concept of an injectable highly porous biodegradable cell delivery system. PLGA(1.6%)/MI2-PNIPAm(3%) dispersion were selected for the remainder of the study because MI2-PNIPAm gave the best combination of cell viability and gel-forming properties. Variable-temperature rheology data for this system were shown in Fig. 5c and d.

Applications such as cardiac tissue repair require gels to withstand strains of up to 20% [36]. The dependence of G' and tan δ on strain at 37 °C was investigated (see Fig. 7). For the dispersions containing PLGA the G' values increased at high strain. A critical strain beyond which G' decreased to less than 95% of the maximum value was identified, γ^*. This corresponds to the onset of network breakdown. Particle gels tend to be more brittle than macromolecular gels [2] and γ^* values less than 1% are common [37]. Remarkably, this was *not* the case for the PLGA/MI2-PNIPAm gels (Fig. 7). The values of γ^* for PLGA(1.6%)/MI2-PNIPAm(3%) and pure MI2-PNIPAm(3%) were 160% and 45%, respectively. For comparison, a dispersion containing a lower MI2-PNIPAm concentration, PLGA(1.6%)/MI2-PNIPAm(1%), had a γ^* value of 100%. It follows that *both* the particles and thermoresponsive polymer cooperatively increase γ^* and promote mechanical flexibility. The data shown in Fig. 7 reveal that unlike conventional particle gels, PLGA/MI2-PNIPAm gels can withstand major strain without breakdown. This is a potential advantage for long term application of this new general class of materials in the body.

The data shown in Fig. 7a shows evidence of strain hardening. Indeed, this requires the presence of PLGA and is strongest for the dispersion containing the highest proportion of PLGA. Strain hardening has been observed for poly(acrylic acid)-*b*-polystyrene star copolymers [38]. Those copolymers bear a structural resemblance to the present MIx-PNIPAm copolymers at temperatures greater than the LCST, i.e., polyelectrolyte centre and hydrophobic arms. However, MIx-PNIPAm is different because strain hardening appears to require the PLGA particles. In order to probe the role of PLGA further the measurements were repeated using only PLGA particles. Those dispersions gave signals that were not distinguishable from the background electrolyte.

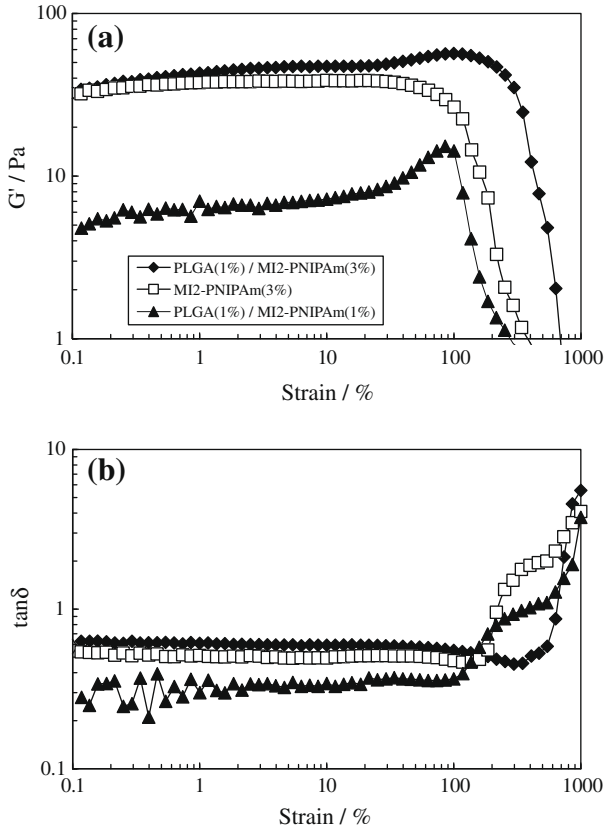

Fig. 7. Variation of G' and tan δ with strain for a PLGA(1.6%)/MI2-PNIPAm(3%) gel at 37 °C compared to a pure copolymer solution. Data for PLGA(1.6%)/MI2-PNIPAm(1%) are also shown for comparison. The data were measured at 10 rad/s.

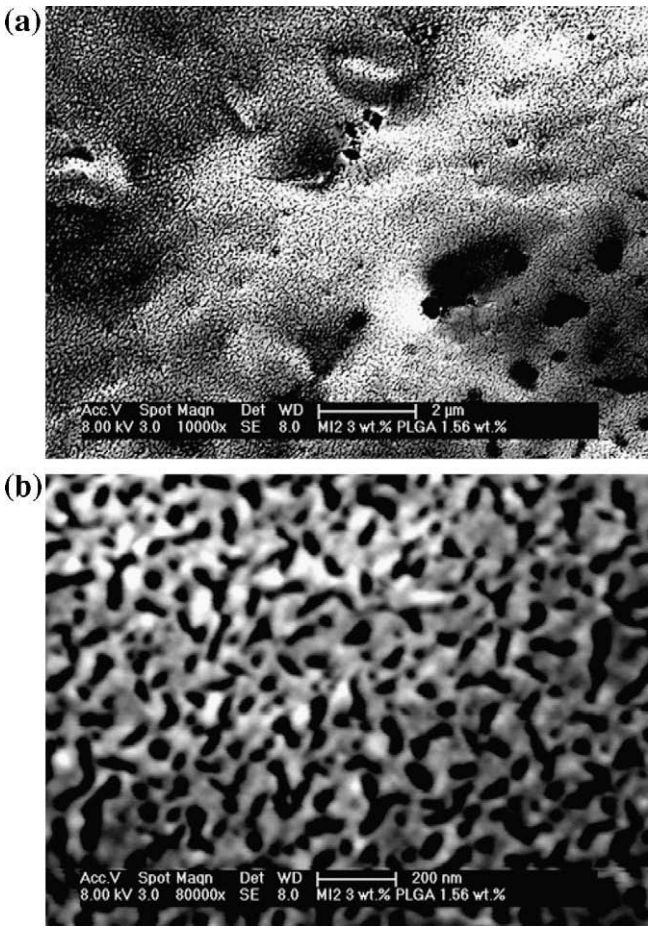

Fig. 8. Representative scanning electron micrographs for a PLGA(1.6%)/MI2-PNIPAm(3%) gel dried at 39 °C obtained at (a) low and (b) high magnification.

Scanning electron micrographs were obtained for a PLGA(1.6%)/MI2-PNIPAm(3%) gel dried in vacuum at 39 °C (see Fig. 8). It can be seen that there is a very high proportion of pores present. Some of these pores have diameters of the order of several micrometres (Fig. 8a). The higher magnification image (Fig. 8b) shows extensively inter-connected elongated pores with pore lengths from about 50 to several 100 s of nanometres are present. The gel network consists of inter-connected strings of copolymer-coated PLGA particles. There was no evidence of the larger particles which were present as a minor component of the particle size distribution (Fig. 1 inset). The morphology present within the *hydrated* gels is assumed to be an expanded version of the morphology shown in Fig. 8. The total porosity of the gel was about 95 vol.% It follows that these gels would allow facile transport of nutrients through the gel if they were able to be used as tissue scaffolds.

Preliminary cell viability studies were conducted using nucleus pulposus cells cultured on the surface of the gels, i.e., two-dimensional cell culture. The live/dead method was used to visualise the cells (Fig. 9). Live and dead cells are green and red, respectively. The systems investigated were PLGA(1.6%)/MI2-PNIPAm(3%) (a–c), pure MI2-PNIPAm(3%) (d–f) and collagen (g–j). The latter was a control gel. The PLGA particles adsorbed the red dye and made visualisation of the cells difficult for the PLGA/MI2-PNIPAm gel (a–c). Nevertheless, viable (green) cells were evident after 6 and 72 h, with more cells visible after 72 h suggesting cell proliferation. All of the cells were adherent and there was some evidence of spreading (Fig. 9c). The latter image shows the spreading expected for the general type of soft gel our dispersions produce [39,40]. Importantly, a high proportion of cells remained viable in the pure MI2-PNIPAm polymer gels. Cell proliferation and spreading was clearly apparent after 72 h (Fig. 9f). This suggests that MI2-PNIPAm has good biocompatibility. However, there appeared to be more cell death (red cells) in the PLGA/MI2-PNIPAm and MI2-PNIPAm gels, when compared to collagen gels, suggesting that these gels are not as biocompatible as collagen. Nevertheless, the data prove the concept that these thermogelling systems can promote cell growth. They provide proof-of-concept data for this new general class of injectable gel-forming biodegradable dispersion which has potential long term potential use as a cell delivery system. Future work will explore three-dimensional injectable constructs, which are beyond the scope of the present study.

3.4. Proposed mechanism for thermoresponsive dispersion behaviour

What are the species within the PLGA/MIx-PNIPAm dispersions that are present at temperatures less than or greater than the LCST? The MIx-PNIPAm copolymers are proposed to resemble flexible star-like copolymers [38]. They comprise a polyelectrolyte centre and thermoresponsive arms (see Fig. 10). They can also associate to a limited extent in solution at temperatures below the LCST. MIx-PNIPAm adsorbs onto the negatively charged PLGA nanoparticles and the neutral PNIPAm arms face the continuous phase with a layer thickness of δ. Because δ is much greater than κ^{-1} (about 9 nm) the zeta potential of the particles approached zero once an adsorbed copolymer layer forms (see Fig. 2a). Some PLGA aggregation also occurs at low temperature, presumably because of the limited tendency for MIx-PNIPAm chains to associate at temperatures less than the LCST. However, all particle–particle interactions become attractive at temperatures greater than the

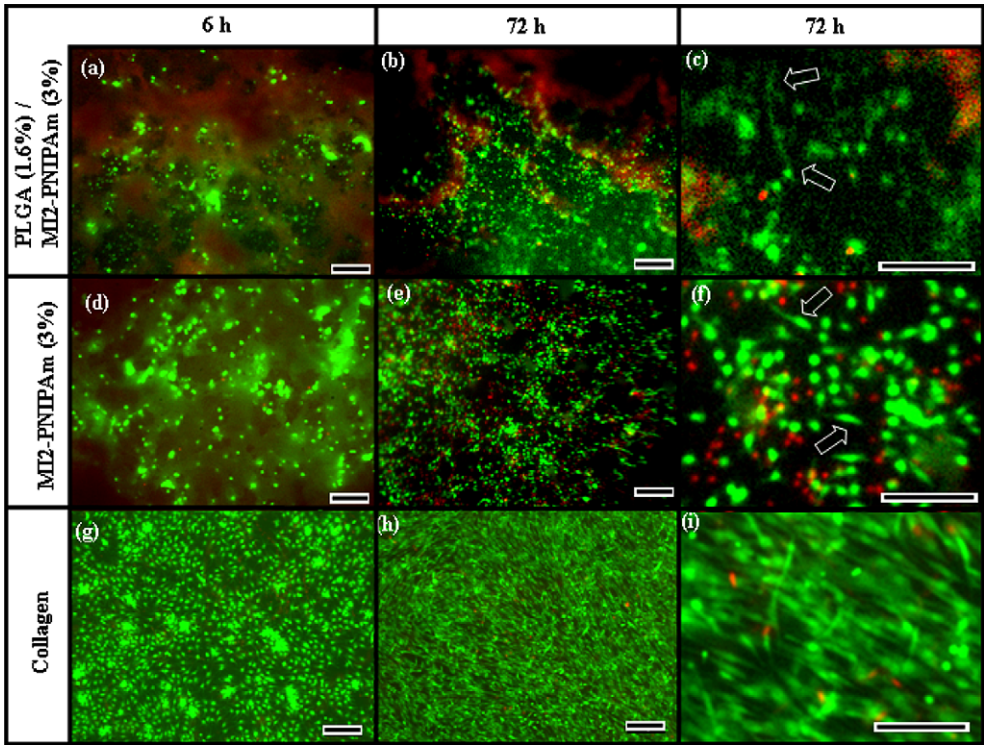

Fig. 9. Fluorescence stereomicroscopy images of stained bovine nucleus pulposus cells cultured on the surface of PLGA(1.6%)/MI2-PNIPAm(3%) (a–c), pure MI2-PNIPAm(3%) (d–f) and collagen (g–i). Cells were fluorescently stained using live (green) and dead (red) dyes. The diffuse red colour shown in (a–c) is due to PLGA particles that have adsorbed the red staining dye. The images were recorded at ca. 37 °C. The culture periods for the cells are indicated. The shorter and longer scale bars represent 200 and 100 μm, respectively. The images shown in (c), (f) and (i) were obtained at high magnification. The arrows show spreading nucleus pulposus cells.

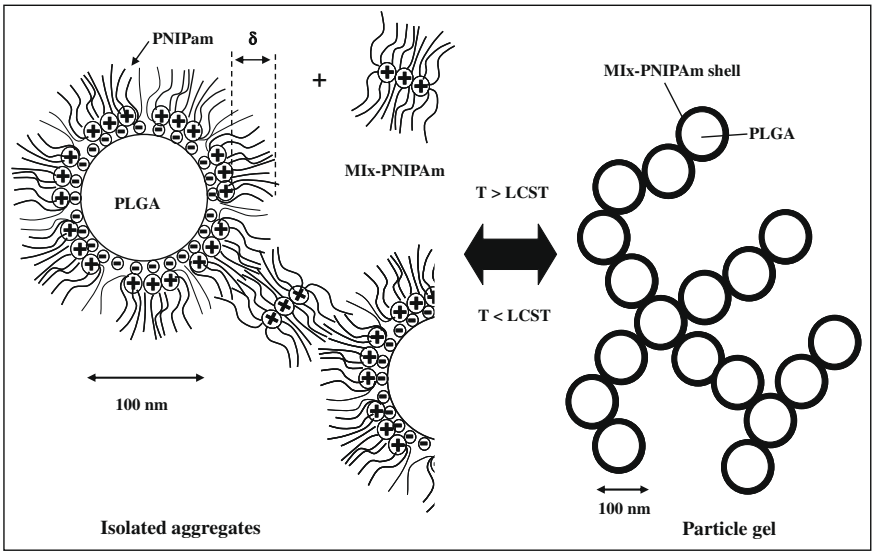

Fig. 10. Schematic diagram showing species proposed to be present within PLGA/MIx-PNIPAm dispersions at temperatures less than or greater than the LCST for MIx-PNIPAm.

LCST and a particle gel forms (see Fig. 10). The particle gels become fluids upon cooling under gentle shear.

4. Conclusions

This study has shown that addition of a cationic graft PNIPAm copolymer to anionic PLGA particles results in a thermoresponsive dispersion. The dilute PLGA/MIx-PNIPAm dispersions undergo thermally-triggered flocculation and the CFT was very close to T_{clpt} for the thermoresponsive copolymer. Concentrated dispersions exhibit thermally-triggered gelation at similar temperatures to T_{clpt}. Importantly, these new gels formed at very low total polymer volume fractions (e.g., less than about 0.05) and were porous at the micrometre and nanometre length scales. A high degree of interconnectivity of the pores was evident. The elasticity of the gels increased with PLGA and copolymer concentration. We aimed to produce a system which gelled at physiological temperatures and this was achieved. Two-dimensional cell viability data showed that PLGA/MI2-PNIPAm

supported nucleus pulposus cell growth for at least 3 days. The data support the view that this general class of PLGA/cationic thermoresponsive copolymer structures may have potential long term use in cell delivery. The ability of the PLGA to hydrolyse could assist gel break down in vivo which could aid its removal by the body. This aspect will be investigated in future work.

Acknowledgments

We gratefully acknowledge the EPSRC for funding this work. We are also grateful to AstraZeneca UK for kindly donating the PLGA used in this study. We thank Chris Thompson and Peter March for access and help with acquiring the microscopy images.

Appendix A. Supplementary material

Supplementary material associated with this article can be found, in the online version, at doi:10.1016/j.jcis.2009.12.030.

References

[1] C. Alava, B.R. Saunders, Langmuir 20 (2004) 3107.
[2] E. Dickinson, J. Chem. Soc., Faraday Trans. 91 (1995) 51.
[3] R. Liu, N. Tirelli, F. Cellesi, B.R. Saunders, Langmuir 25 (2009) 490–496.
[4] E. Dickinson, J. Colloid. Interface Sci. 225 (2000) 2.
[5] D. Durand, J.G. Gimel, T. Nicolai, Physica A 304 (2002) 253.
[6] W. Wang, H. Liang, R. Cheikh Al Ghanami, L. Hamilton, M. Fraylich, K.M. Shakesheff, B.R. Saunders, C.A. Alexander, Adv. Mater. 21 (2009) 1809.
[7] I. Naoyuki, S. Biggs, Macromolecules 40 (2007) 9045.
[8] A. Durand, D. Hourdet, Polymer 41 (2000) 545.
[9] A. Durand, D. Hourdet, F. Lafuma, J. Phys. Chem. B 104 (2000) 9371.
[10] R. Liu, M. Fraylich, B.R. Saunders, Colloid Polym. Sci. 287 (2009) 627.
[11] A. Koh, B.R. Saunders, Langmuir 21 (2005) 6734.
[12] C. Alava, B.R. Saunders, Colloid Surf., A 270 (2005) 18.
[13] K.E. Uhrich, S.M. Cannizzaro, R.S. Langer, K.M. Shakesheff, Chem. Rev. 99 (1999) 3181.
[14] H. Okada, Adv. Drug Delivery Rev. 28 (1997) 43.
[15] H. Fessi, F. Puisieux, J.P. Devissaguet, N. Ammoury, S. Benita, Int. J. Pharm. 55 (1989) R1.
[16] S. Galindo-Rodriguez, E. Allemann, H. Fessi, E. Doelker, Pharm. Res. 21 (2004) 1428.
[17] M. Fraylich, W. Wang, K. Shakesheff, C. Alexander, B. Saunders, Langmuir 24 (15) (2008) 7761–7768.
[18] R. Liu, P. De Leonardis, F. Cellesi, N. Tirelli, B.R. Saunders, Langmuir 24 (2008) 7099.
[19] R. Liu, F. Cellesi, N. Tirelli, B.R. Saunders, Polymer 50 (2009) 1456–1462.
[20] S. Levenberg, R. Langer, Curr. Top. Dev. Biol. 61 (2004) 113.
[21] R.C. Weast, D.R. Lide, M.J. Astle, W.H. Beyer, Handbook of Chemistry and Physics, 70th ed., CRC Press 1916, Florida, 1989.
[22] X.Y. Chen, S.P. Armes, Adv. Mater. 15 (2003) 1558.
[23] S.E. Dunn, A.G.A. Coombes, M.C. Garnett, S.S. Davis, M.C. Davies, L. Illum, J. Controlled Release 44 (1997) 65.
[24] J.A. Long, D.W.J. Osmond, B. Vincent, J. Colloid Interface Sci. 42 (1973) 545.
[25] E. Daly, B.R. Saunders, Langmuir 16 (2000) 5546.
[26] D.H. Everett, Basic Principles of Colloid Science, RSC, London, 1988.
[27] D.J. Shaw, Colloid and Surface Chemistry, fourth ed., Butterworth-Heinemann, Oxford, 1992.
[28] K. Furusawa, S. Satou, Colloid Surf., A 195 (2001) 143.
[29] P.F. Luckham, M.A. Ukeje, J. Colloid Interface Sci. 220 (1999) 347.
[30] M.L. Houchin, E.M. Topp, J. Appl. Polym. Sci. 114 (2009) 2848.
[31] J.W. Goodwin, R.W. Hughes, Rheology for Chemists: An Introduction, RSC Press, Cambridge, 2000.
[32] M. Whittle, E. Dickinson, J. Chem. Soc., Faraday Trans. 94 (1998) 2453.
[33] D. Shaw, Introduction to Colloid and Surface Chemistry, fourth ed., Butterworth Heinemann, 1996.
[34] H. Tanii, K. Hashimoto, Toxicol. Lett. 58 (1991) 209.
[35] I. Vyas, H.E. Lowndes, R.D. Howland, Neurotoxicology 6 (1985) 123.
[36] Q.-Z. Chen, S.E. Harding, N.N. Ali, A.R. Lyon, A.R. Boccaccini, Mater. Sci. Eng., R 59 (2008) 1.
[37] A. Chougnet, A. Audibert, M. Moan, Rheol. Acta 46 (2007) 793.
[38] S. Hietala, S. Strandman, P. Jarvi, M. Torkkeli, K. Jankova, S. Hvilsted, H. Tenhu, Macromolecules 42 (2009) 1726.
[39] G. Bao, S. Suresh, Nat. Mater. 2 (2003) 715.
[40] C. Zhu, G. Bao, N. Wang, Ann. Rev. Biomed. Eng. 2 (2000) 189.